Supplement to: Highly aggregated antibody therapeutics can enhance the *in vitro* innate and late-stage T-cell immune responses

Table of Contents

Supplemental Text:

Aggregates Induce T-cell Adaptive Responses-In the T-cell adaptive response, aggregation of mAb2 induced a higher response than the monomeric form. This response was attributed to the aggregation rather than the inherent immunogenic potential of the molecule. As further support of this, we tested two additional molecules with high and low rates of clinical immunogenicity and found that a higher T-cell response was induced upon aggregation for both molecules (data not shown). This indicates that the aggregation of a mAb might drive the activation of T-cells in PBMC independent of the intrinsic immunogenic potential. Further evaluation of the cell types responsible and the evaluation of antigen specificity of these responses will help to address these observations.

Aggregates Induce IL-10 Secretion from PBMC-IL-10 secretion from PBMC in response to aggregates was also tested by IL-10 ELISPOT, in order to track the release of this mechanistically important cytokine as well as enumerate cytokine secreting cells. PBMC were challenged with mAb1 and mAb3 monomeric and aggregated samples and assessed at the innate phase (20 h). Most aggregated samples were found to increase the average SI of responding donors (SI > 2.0) and the % donors that responded above the relevant mAb monomer (supplemental Fig. 1). Interestingly, the detection of the immunosuppressive cytokine IL-10 at the innate phase may implicate immunological tolerance, leading to the generation of aggregate-specific tolerance in memory T-cells. Interestingly, the detection of the immunosuppressive cytokine IL-10 at the innate phase may suggest effects on antigen presentation and maturation of APC such as dendritic cells and down regulation of cytokine production, leading to the generation of aggregate-specific tolerance in memory T-cells (66,67).

Supplemental Experimental Procedures:

PBMC Preparation-Human PBMC from healthy naïve donors were obtained from Amgen's environmental health and services department (EH&S), as previously described (39). Briefly, PBMC were isolated for functional assays using vacutainer cell preparation tubes (BD Diagnostics) containing sodium heparin. The tubes were centrifuged for 30 min at 20°C at 1600xg. Plasma and PBMC were collected in 15 mL conical tubes and centrifuged for 15 minutes at 300xg. The cell pellet was resuspended and washed twice with PBS and cryopreserved in freezing medium (Human AB serum with 10% DMSO). HLA-DR haplotyping was performed on all donors as previously described (39). Prior to the various assays, frozen PBMC were thawed using growth media at 37^{o}C containing 89% RPMI, 10% Human AB serum and 1% penicillin/streptomycin/glutamine. The cells were counted and assessed for viability using Trypan Blue stain using a Cellometer (Nexcelom Biosciences LLC). Thawed cells that had a viability of 85% and above were used in the functional assays.

Multiplex Cytokine Analysis-Multiplexed cytokine analysis was performed on culture supernatants by Luminex using MILLIPLEX human panel kits (EMD Millipore) containing relevant standards and quality controls, according to the manufacturer's instructions. For analysis of the PBMC supernatants at 20 h, the following 17 cytokines were tested: GM-CSF, IFN-γ, IL-1β, IL-1ra, IL-2, IL-4, IL-5, IL-6, IL-8, IL-10, IL-12p40, IL-12p70, MCP-1, MIP-1α, MIP-1β, TNF-α, and TNF-β. Only select cytokine data is shown. Analysis was performed by a Luminex FlexMAP 3D instrument with xPonent version 4.0 software. The Milliplex Analyst version 3.5.5.0 software was used to convert the mean fluorescent intensity data reported to a cytokine/chemokine concentration (pg/mL) using a standard curve and a five-parameter curve fitting model.

For some experiments, culture supernatants were tested with either the Human InflammationMAP v1.0, Human CytokineMAP A v1.0 or Human CytokineMAP B v1.0 (Myriad RBM, Austin, TX). The least detectable dose (LDD) was determined as the mean + 3 SDs of 20 blank readings. All values below the LDD were assigned a value equal to the LDD for subsequent calculations.

Biophysical Characterization-Aggregated solutions were biophysically assessed for particle number and changes in secondary structure as described in our previous report (26). In brief, nanoparticle tracking analysis was performed on a NanoSight LM10-HSB (NanoSight, Amesbury, UK), containing a high sensitivity EMCCD camera and 405 nm blue laser. Aggregated samples made at 1 mg/mL were diluted 10 fold, injected into the sample chamber, and videos were recorded. The NanoSight NTA version 2.0 Build 0252 software was used for data analysis. For particle detection in the micron and visible ranges, aggregated samples made at 1 mg/mL were diluted (20-440x), degassed, and then analyzed by the appropriate instrument. Particle counting and size distribution in the micron size range was achieved on a HIAC/Royco liquid particle counter model 9703 with an HRLD-150 sensor and the software PharmSpec (HACH Ultra Analytics, Grants Pass, OR). Particle imaging in the micron and visible size range (≥ 125 μm) was achieved by a liquid-borne particle Micro-Flow Imaging System DPA4100 (Brightwell Technologies, Inc.). All final particle numbers were adjusted for the initial dilution factor.

Secondary structural changes were detected by comparing the fourier transform infrared (FTIR) spectra of the monomeric and aggregated samples obtained with the Vertex 70 FT-IR spectrophotometer with the attenuated total reflectance device and OPUS spectroscopy software version 6.5 (Bruker Optics) (26). Aggregated sample spectra were compared against the

monomeric sample in the second derivative amide I region, 1600-1700 wavenumber cm^{-1}, except for the mAb1-microspheres which were compared between 1620-1700 wavenumber cm^{-1} to minimize interference due to the spectra by the microspheres themselves. The correlation coefficient (CC) was calculated using the Thermal Electron OMNIC software version 5.1b (Nicolet Instrument Corp) (68), where a correlation value of ≥ 93% indicates an identical match (69).

IL-10 ELISPOT-IL-10 ELISPOT was conducted according to the manufacturer's instructions (BD Pharmingen). Briefly, thawed PBMC from 10 donors were added at a concentration of 3×10^6 PBMC/mL to a 96-well ELISPOT plate and then challenged with 40 μg/mL of the monomeric or aggregated samples. Conditions testing stress-treated buffer, no cells, media-only, and LPS were also included. Plates were processed 20 h after incubation according the manufacturer, and IL-10 secreting cells were counted on an AID EliSpot Reader System with accompanying version 5.0 software. The SI was calculated as the number of spots per well (spw) for donors treated with aggregated mAbs divided by the number of spw for donors treated with monomeric mAbs. An SI > 2.0 was considered positive.

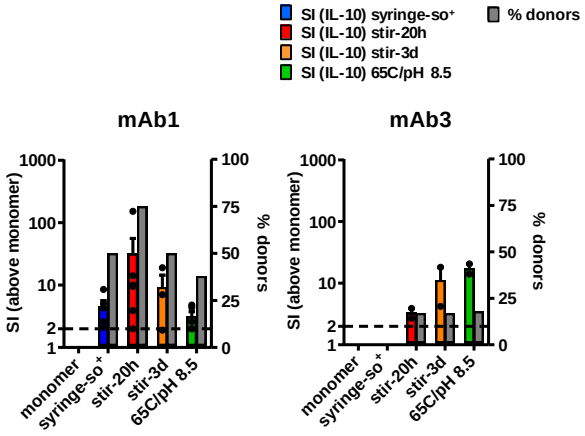

Supplemental Figure 1. Aggregation of mAbs enhances the secretion of IL-10 from PBMC. PBMC from 6-10 donors were tested for IL-10 secretion by ELISPOT in response to aggregated mAbs. The average SI of positive donors (SI > 2.0) above the response to the relevant monomeric mAb is shown.

Supplemental References:

66. De Smedt, T., Van Mechelen, M., De Becker, G., Urbain, J., Leo, O., and Moser, M. (1997) *Eur J Immunol* 27, 1229-1235
67. Fiorentino, D. F., Zlotnik, A., Mosmann, T. R., Howard, M., and O'Garra, A. (1991) *J Immunol* 147, 3815-3822
68. Cover, T. M., and Hart, P. E. (1967) *IEEE Transactions on Information Theory* Vol. IT-13, 21-27
69. Jiang, Y., Li, C., Nguyen, X., Muzammil, S., Towers, E., Gabrielson, J., and Narhi, L. (2011) *J Pharm Sci* 100, 4631-4641